

# Iterative Deconvolution-Interpolation Gridding

R. E. Gabr<sup>1</sup>, P. Aksit<sup>2</sup>, P. A. Bottomley<sup>1,3</sup>, A. M. Youssef<sup>4</sup>, Y. M. Kadah<sup>4</sup>

<sup>1</sup>Department of Electrical and Computer Engineering, Johns Hopkins University, Baltimore, MD, United States, <sup>2</sup>Global Applied Science Laboratory, GE Healthcare, Waukesha, WI, United States, <sup>3</sup>Division of MR Research, Johns Hopkins University, Baltimore, MD, United States, <sup>4</sup>Department of Biomedical Engineering and systems, Cairo University, Giza, Egypt

## Introduction

A convolution-interpolation algorithm—the *gridding algorithm*—is widely used to reconstruct images from nonuniform samples in k-space. The gridding algorithm consists of: (1) compensating the data for nonuniform sampling by multiplying by a suitable sampling density compensation function (DCF); (2) convolving the compensated data with a small-width kernel sampling the result onto a rectilinear grid; (3) Fourier transform (FT) the data into image space; and (4) compensating for signal roll-off introduced by the convolution, by dividing by the FT of the convolution window [1]. Although this algorithm is efficient and stable, it is non-optimal and artifact-prone [2]. Calculation of the optimal DCF has proved a difficult and long-standing problem, and step (4) results in large signal wings at the image periphery. Other gridding solutions often include truncation and/or approximations that affect reconstruction accuracy in a non-deterministic way, such as the BURS method [3]. Moreover, the calculation of gridding coefficients and/or the DCF is almost always computationally exhaustive [3,4] or requires regularization [3]. This is intolerable in situations where the k-space trajectory must be changed. Here, we present a more accurate, yet simple, solution. Instead of the convolution-interpolation operation which depends on the DCF used, a deconvolution-interpolation process is performed that is more accurate and does not need density compensation. The deconvolution is implemented by solving a sparse linear system using the conjugate gradient (CG) method.

## Theory

Let  $M$  be the continuous FT of the object to be imaged. Assume that k-space is well-covered by the sampling trajectory and the imaged object is of finite-support. The nonuniform samples are related to the data on the grid with a sinc-function interpolation, that is,

$M(\mathbf{k}_j) = \sum_n M(\mathbf{k}_n) \text{sinc}(\mathbf{l}\mathbf{k}_j - \mathbf{k}_n)$ , where  $\{\mathbf{k}_j\}_{j=1..L}$  are the  $L$  trajectory sampling locations and  $\{\mathbf{k}_n\}_{n=1..N}$  are the  $N$  sampling grid points. Stacking the nonuniform and uniform samples in column vectors  $\mathbf{m}_s$  and  $\mathbf{m}$ , respectively, the interpolation can be written in a matrix form as  $\mathbf{m}_s = \mathbf{A}\mathbf{m}$ , where the dense matrix  $\mathbf{A}$  contains the *sinc* interpolation coefficients. Solving for  $\mathbf{m}$  is impractical as the size of  $\mathbf{A}$  is prohibitively large. However, replacing the infinite *sinc* function with a small convolution window, yields the sparse linear system,  $\mathbf{m}_s = \mathbf{C}\mathbf{m}_r$ , where  $\mathbf{C}$  is an interpolation matrix with a small-width kernel  $C(\mathbf{k})$  and  $\mathbf{m}_r$  is a vector of uniform samples.

This interpolation is accurate since it is performed on a uniform grid. This linear system can be inverted efficiently using the CG method, since  $\mathbf{C}$  is sparse. The inversion is essentially a deconvolution of  $M(\mathbf{k})$  with the convolution kernel  $C(\mathbf{k})$  sampling the result onto a rectilinear grid. The same sparse-system formulation has been used previously with a quite different system matrix [4]. The relationship between  $\mathbf{m}_r$  and the desired true object  $\mathbf{m}$  is the weighting by  $1/c(\mathbf{r})$  caused by the deconvolution, where  $c(\mathbf{r})$  is the FT of  $C(\mathbf{k})$  and  $\mathbf{r}$  is the position vector in image space. This effect is eliminated by multiplying in the central part by  $c(\mathbf{r})$ .

## Experiments

Axial gradient-echo spiral scans of healthy volunteers were done on a 1.5T GE CV/i system (GE Healthcare, Waukesha WI; 32 spiral with 4096 samples each; 24 cm FOV; 5mm slices; TR/TE = 51/2.5 ms; 60° flip angle). Images were reconstructed onto a 512x512 grid with a Kaiser-Bessel window (width=3 rectilinear grid points; optimal beta parameters) [1]. Conventional gridding was implemented with  $DCF(\mathbf{K}_j) = \mathbf{g}_j \cdot \mathbf{K}_j$  where  $\mathbf{g}_j = (g_{xj}, g_{yj})$  is the gradient vector at  $\mathbf{k}_j$ . The same window was used for the new method but with a beta parameter of 8.3. Fig. 1 shows *in vivo* brain images reconstructed with conventional and new gridding algorithms. Artifacts at the periphery of the conventionally gridded image are absent with the new method. The signal-to-artifact ratio (SARR), defined as the mean signal in a region of interest over the standard deviation in a background region (Fig. 1), is higher at 36.7 for the new algorithm, vs 32.1 by the conventional method. Within the brain, no difference in intensity levels is evident. Ten iterations were sufficient to achieve a convergent solution.

## Conclusions

The new algorithm provides accurate image reconstruction from arbitrary k-space trajectories without grid subsampling, as is required in other methods [1,5]. This saves memory and allows smaller FOV and increased resolution. Density compensation is embedded in the deconvolution step. The inherent regularization in the CG method assures stability of the deconvolution process. Construction of the gridding matrix is simple and fast and no regularization is needed. This is useful for changing k-space trajectories.

## References

- [1] J. I. Jackson et al., IEEE Trans Med Imag, 10 (1991) 472–478. [2] H. Schomberg et al. IEEE Trans Med Imag 14 (1995) 596–607.  
[3] D. Rosenfeld, Magn Reson Med 48 (2002) 193–202. [4] Y. M. Kadah, Proc. SPIE Med Imag, 2002, 84–92.  
[5] H. Moriguchi, J.L. Duerk, Magn Reson Med 2004; 51:343–352. Supported in part by NIH grant R01 RR15396

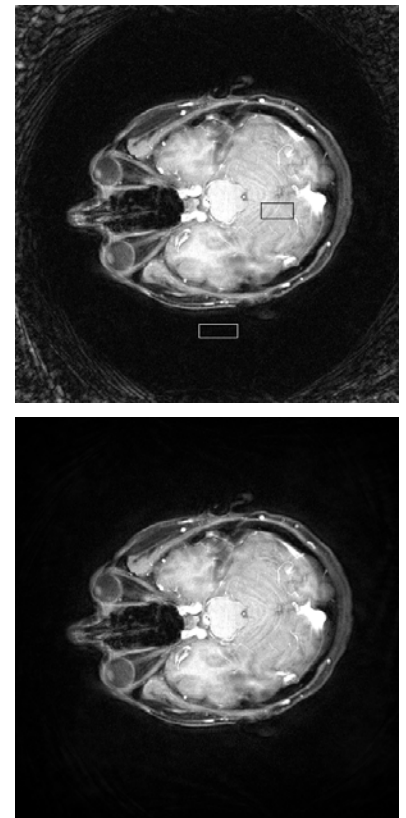


**Fig. 1** Spiral images reconstructed with conventional gridding (top) and new algorithm (bottom). Boxes show areas in/outside head used for SARR.